Journal of Pathology
J Pathol 2011; **224:** 33–44
Published online 22 March 2011 in Wiley Online Library (wileyonlinelibrary.com) DOI: 10.1002/path.2840

ORIGINAL PAPER

Fibrillin-1 genetic deficiency leads to pathological ageing of arteries in mice

Boubacar Mariko,[1] Mylène Pezet,[2] Brigitte Escoubet,[3] Stéphanie Bouillot,[1] Jean-Pierre Andrieu,[4] Barry Starcher,[5] Daniela Quaglino,[6] Marie-Paule Jacob,[7] Philippe Huber,[1] Francesco Ramirez[8] and Gilles Faury[1]*

[1] *(i) Université Joseph Fourier, Grenoble, F-38041, France; (ii) CEA, Grenoble, F-38054, France; (iii) INSERM, U882, Grenoble, F-38054, France*
[2] *INSERM, CEFI-IFR2, Paris, F-75018, France*
[3] *(i) INSERM, U872, Paris, F-75006, France; (ii) Assistance-Publique-Hopitaux de Paris-Hôpital Bichat, Service de Physiologie, Paris, F-75018, France; (iii) Université Paris 7, Faculté de Médecine Denis Diderot, Paris, F-75018, France; (iv) INSERM, CEFI-IFR2, Paris, F-75018, France*
[4] *Laboratoire d'Enzymologie Moléculaire, Institut de Biologie Structurale, Université Joseph Fourier—CEA, Grenoble, France*
[5] *Department of Biomedical Research, University of Texas Health Center, Tyler, Texas, USA*
[6] *Department of Biomedical Sciences, University of Modena and Reggio Emilia, Modena, Italy*
[7] *(i) INSERM, U698, Paris, F-75877, France; (ii) Hôpital Bichat-Claude Bernard, Paris, F-75877, France*
[8] *Department of Pharmacology and Systems Therapeutics, Mount Sinai School of Medicine, New York, NY, USA*

**Correspondence to: Gilles Faury, iRTSV-APV, CEA-Grenoble, 17 Rue des Martyrs, 38 054 Grenoble Cedex 9, France.*
e-mail: Gilles.Faury@ujf-grenoble.fr

Abstract

Fibrillin-1, the major component of extracellular microfibrils that associate with insoluble elastin in elastic fibres, is mainly synthesized during development and postnatal growth and is believed to guide elastogenesis. Mutations in the fibrillin-1 gene cause Marfan syndrome, a multisystem disorder characterized by aortic aneurysms and dissections. The recent finding that early deficiency of elastin modifies vascular ageing has raised the possibility that fibrillin-1 deficiency could also contribute to late-onset pathology of vascular remodelling. To address this question, we examined cardiovascular function in 3-week-old, 6-month-old, and 24-month-old mice that are heterozygous for a hypomorphic structural mutation of fibrillin-1 (*Fbn1*$^{+/mg\Delta}$ mice). Our results indicate that *Fbn1*$^{+/mg\Delta}$ mice, particularly those that are 24 months old, are slightly more hypotensive than wild-type littermates. Additionally, aneurysm and aortic insufficiency were more frequently observed in ageing *Fbn1*$^{+/mg\Delta}$ mice than in the wild-type counterparts. We also noted substantial fragmentation and decreased number of elastic lamellae in the aortic wall of *Fbn1*$^{+/mg\Delta}$ mice, which were correlated with an increase in aortic stiffness, a decrease in vasoreactivity, altered expression of elastic fibre-related genes, including fibrillin-1 and elastin, and a decrease in the relative ratio between tissue elastin and collagen. Collectively, our findings suggest that the heterozygous mgΔ mutation accelerates some aspects of vascular ageing and eventually leads to aortic manifestations resembling those of Marfan syndrome. Importantly, our data also indicate that vascular abnormalities in *Fbn1*$^{+/mg\Delta}$ mice are opposite to those induced by elastin haploinsufficiency during ageing that affect blood pressure, vascular dimensions, and number of elastic lamellae.

Keywords: elastic lamellae; fibrillin-1; Marfan syndrome; arterial ageing; aneurysm; transgenic mice

Received 18 May 2010; Revised 11 November 2010; Accepted 6 December 2010

No conflicts of interest were declared.

Introduction

Elasticity is a vital physiological property of large arteries. During systole, pressurized blood dilates large arteries, while elastic components of the arterial wall store energy. During diastole, the arterial wall releases the accumulated energy by compressing the blood, therefore maintaining blood pressure and flow into the arterial tree [1]. Circumferentially oriented elastic lamellae made of elastin and microfibrils fulfil this function in the closed circulatory system of higher vertebrates, whereas microfibrils devoid of elastin are the sole elastic components of invertebrate arteries owing to their limited stretching in response to mechanical force [2,3]. Microfibrils are macromolecular structures that are mainly composed of fibrillin-1 and which also include microfibril-associated glycoproteins (MAGPs), latent TGF-β-binding proteins (LTBPs), and fibulins [4]. Despite their relatively low abundance (~10% compared with elastin), microfibrils exert a significant mechanical function in the elastic fibres of large arteries, as evidenced by the vascular manifestations of fibrillin-1 mutations in Marfan syndrome (MFS), which include increased arterial stiffness and abnormal aortic wall architecture that precipitate dissecting aneurysms [5–10].

Elastic fibres undergo a slow age-dependent degradation due to the progressive imbalance between elastolytic enzymes and their inhibitors, leading to the release of elastin peptides with vasodilatory properties [11–13]. In accordance with these findings, genetic elastin deficiency was recently shown to modify the physiological process of arterial ageing in $Eln^{+/-}$ mice [14]. As already alluded to, several mouse strains with discrete *Fbn1* mutations have been created that replicate the clinical spectrum of MFS, including aneurysmal pathologies that manifest during neonatal or adult life [15–18]. Amongst them is the so-called mgΔ mutation, a hypomorphic in-frame deletion of exons 19–24 of *Fbn1*, which in homozygosity causes dissecting aneurysm and death soon after birth but has no apparent effect on the viability and fitness of young heterozygous mutant mice [17]. The present study employed $Fbn1^{+/mg\Delta}$ mice to investigate whether fibrillin-1 may also contribute to cardiovascular function during ageing. The results of these analyses revealed that the *Fbn1* mutation promotes several negative changes in cardiovascular function as the mouse ages, including an increased rate of aortic aneurysm and rupture.

Materials and methods

Animals

The present study employed mice heterozygous for a hypomorphic in-frame deletion in fibrillin-1 ($Fbn1^{+/mg\Delta}$), which were backcrossed for more than five generations into the C57Bl/6J background [17]. The analyses were performed on male $Fbn1^{+/mg\Delta}$ mice and wild-type (WT) littermates (controls) of three age groups: 3-week-old (young animals), 5- to 7-month-old (adult animals, called 6-month-old), and 23- to 27-month-old (old animals, called 24-month-old). No change in neonatal mortality was observed in $Fbn1^{+/mg\Delta}$ mice compared with WT littermates. Housing and surgical procedures were in accordance with institutional guidelines.

Blood pressure and heart weight

Mice were anaesthetized using isoflurane (1.5–2%) and placed on a heating table to maintain body temperature at 37 °C. Immediately after completion of anaesthesia, verified by the absence of a response to pinching of the mouse toes, a Millar SPR838 probe was inserted into the carotid artery and then moved to the ascending aorta, where the blood pressure was measured. In other animals, anaesthetized with pentobarbital (60 mg/kg, intraperitoneally), hearts and left ventricles were dissected, washed, and weighed (wet weight).

Ultrasound

Transthoracic echocardiography was performed with a Toshiba Powervision 6000, SSA 370A device equipped with an 8- to 14-MHz linear transducer, as previously described [19,20]. Procedures are described in detail in the Supporting information, Supplementary methods.

Arterial desmosine and hydroxyproline content

Desmosine was determined by radioimmunoassay, as previously described [21]. Total protein in the tissue hydrolysates was determined by a ninhydrin-based method [22]. Hydroxyproline levels were determined by amino acid analysis using high-pressure ion-exchange chromatography on a Biochrom 30 (Biochrom, Cambridge, UK) amino acid analyser. Norleucin was used as an internal standard. Results are expressed as amino acid mass per vessel segment length and as amino acid mass per vessel total protein content.

Aorta mechanics

Mechanical studies were performed on excised cannulated ascending aortae, as described [14,23]. Procedures are described in detail in the Supporting information, Supplementary methods.

Histological analyses

Aortae were classified as aneurysmal/symptomatic when obvious dilation of a vessel section was observed by gross anatomy/visual examination. Transverse sections of the paraffin-embedded ascending aorta (pathological or non-pathological) were stained with haematoxylin and eosin for cells, Weigert for elastic fibres, and picrosirius red for collagen. Some aortae were fixed by cardiac perfusion with 2.5% glutaraldehyde in 0.1 M sodium cacodylate buffer (pH 7.4) and then embedded in Epon for ultrastructural analyses. Semi-thin sections were stained as previously described [24] and stained with tannic acid before uranyl acetate.

RNA analyses

Total RNA was extracted from entire aortae, and gene expression levels were evaluated by real-time PCR. Resulting values were normalized against the expression of the housekeeping gene hypoxanthine guanine phosphoribosyl transferase (HPRT) and total mRNA input. Amplification primers for the tested genes have been previously described [14]. Procedures are described in detail in the Supporting information, Supplementary methods.

Aorta reactivity

Variations of cannulated aorta diameters in response to 10 µmol/l of the vasoconstrictor phenylephrine (PE) and then 10 µmol/l PE + 10 µmol/l of the vasodilator acetylcholine (Ach) were assessed at 75 mmHg [14,23]. Diameters of $Fbn1^{+/mg\Delta}$ mouse aortae were normalized against the mean diameter of WT aortae [11].

Statistics

Two- or three-way ANOVA followed, when necessary, by Fisher's least significant difference (LSD) test or *t*-test for paired value comparisons, was used to evaluate the significance of most parameters. The non-parametric Mann–Whitney *U*-test was used to assess vessel mid-wall strain, stress, incremental elasticity modulus, and distensibility. The results are presented as mean values ± standard error of the mean (SEM). p values less than or equal to 0.05 were considered statistically significant.

Results

The mgΔ allele encodes a shortened fibrillin-1 molecule that is produced at ∼10% of the normal level [17]. Previous investigations showed that newborn *Fbn1*$^{mg\Delta/mg\Delta}$ mice succumb to cardiovascular and/or respiratory complications, but did not determine whether seemingly normal *Fbn1*$^{+/mg\Delta}$ mice display cardiovascular manifestations past their reproductive age [17,25]. In the present study, we noted a statistically borderline loss of *Fbn1*$^{+/mg\Delta}$ viability only between 12 and 20 months of age ($p = 0.06$; χ^2 test at 18 months) in the absence of substantial changes in body weight (Figure 1A and Table 1). We also found lower blood pressures and higher pulse pressure in *Fbn1*$^{+/mg\Delta}$ mice compared with WT littermates (three-way ANOVA, $p \leq 0.05$; Table 1), conceivably as a result of aortic insufficiency in *Fbn1*$^{+/mg\Delta}$ mice (see below). As shown in a previous study in which blood pressure was found to be similar in awake or anaesthetized mice, an effect of anaesthesia explaining this inter-group difference could not be suspected [23]. Hence, several critical parameters of cardiovascular physiology were compared between young (3-week-old), adult (6-month-old), and old (24-month-old) *Fbn1*$^{+/mg\Delta}$ and *WT* mice.

Cardiovascular function

Ultrasound measurements through the cardiac cycle of ascending aortae in adult *Fbn1*$^{+/mg\Delta}$ mice revealed increases of 38% and 71% in diastolic diameter and aortic surface, respectively (Table 1 and Supporting information, Supplementary Figure 1A). The unusual presence of aortic aneurysm was also noted in 31% (4 out of 13) of adult *Fbn1*$^{+/mg\Delta}$ mice (versus 7% in adult *Fbn1*$^{+/+}$ animals; 1 out of 15), which reached a significantly greater frequency than normal (67% or 8 out of 12 mice) in old *Fbn1*$^{+/mg\Delta}$ mice (versus 17% in aged *Fbn1*$^{+/+}$ animals; 2 out of 12) (Figure 1B). Additionally, aortic compliance (estimated from the ratio of the diameters and pressure gradients between systole and diastole) was reduced in some, but not all, adult mutant animals, leading to a non-significant trend towards decreased compliance in this group (Table 1). Retrograde flow (measured using colour-Doppler mode) was

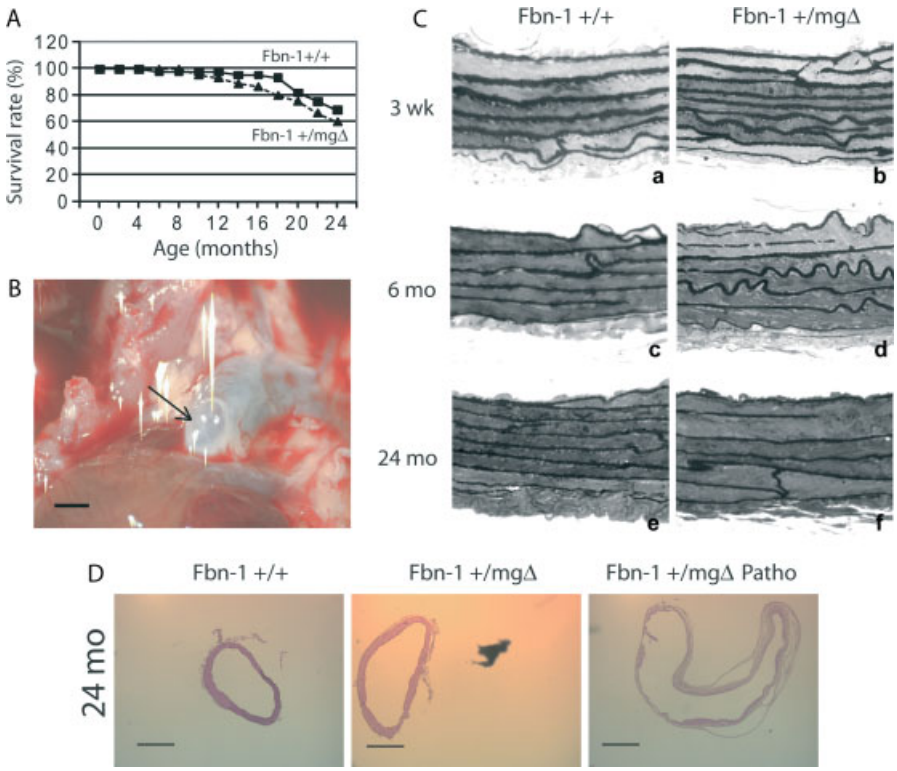

Figure 1. Effect of ageing and genotype on the survival rate (A), aneurysmal ascending aorta of a 24-month-old *Fbn1*$^{+/mg\Delta}$ mouse (B) (the arrow indicates the saccular aneurysm at the vessel root), and histological examination of semi-thin sections of ascending aorta of 3-week-old and 6- and 24-month-old mice (C). Eosin/haematoxylin staining of cross-sections of ascending aorta of *Fbn1*$^{+/+}$, non-pathological *Fbn1*$^{+/mg\Delta}$, and pathological *Fbn1*$^{+/mg\Delta}$ (Patho) 24-month-old mice (D). $n = 45$ for A. Bar sizes: 1 mm (B) and 500 µm (D).

Table 1. Haemodynamic and ultrasound parameters of ascending aorta and heart

	5- to 7-month-old		23- to 27-month-old	
	Fbn1$^{+/+}$	*Fbn1*$^{+/mg\Delta}$	*Fbn1*$^{+/+}$	*Fbn1*$^{+/mg\Delta}$
Number of animals	8	8	7	5
Body weight (BW) (g)	29.5 ± 0.9	31.8 ± 0.7*	33.2 ± 1.3†	31.6 ± 0.8
Entire heart weight/BW (mg/g)	4.92 ± 0.13	5.99 ± 0.91	5.72 ± 0.35	6.25 ± 0.94
Systolic arterial pressure (mmHg)	105 ± 2	104 ± 3	110 ± 4	104 ± 5
Mean arterial pressure (mmHg)	85 ± 1	81 ± 2	84 ± 3	76 ± 6
Diastolic arterial pressure (mmHg)	75 ± 1	70 ± 2	72 ± 3	62 ± 6
Pulse pressure (mmHg)	30 ± 1	34 ± 3	38 ± 3	42 ± 2
Ultrasound study				
Ascending aorta				
Systolic diameter (mm)	1.70 ± 0.05	2.18 ± 0.17*	2.11 ± 0.07†	2.26 ± 0.19*
Diastolic diameter (mm)	1.48 ± 0.04	2.04 ± 0.19*	1.97 ± 0.08†	2.05 ± 0.21*
Surface (mm^2)	2.28 ± 0.14	3.90 ± 0.66*	3.53 ± 0.22†	4.09 ± 0.66
Compliance (mm/mmHg)	0.720 ± 0.137	0.520 ± 0.112	0.383 ± 0.07‡	0.579 ± 0.173
Cardiac data				
Heart rate (bpm)	504 ± 11	485 ± 25	475 ± 16	456 ± 22
Left atria dimension (mm)	2.7 ± 0.1	2.7 ± 0.1	2.7 ± 0.1	2.9 ± 0.4
LVEDD	4.36 ± 0.18	5.00 ± 0.54	5.13 ± 0.15†	5.11 ± 0.26
LVEDD/BW (mm/g)	0.148 ± 0.005	0.158 ± 0.017	0.156 ± 0.008	0.162 ± 0.011
Fractional shortening (%)	40 ± 2	31 ± 4	36 ± 3	35 ± 4
LV weight/BW (mg/g)	3.58 ± 0.20	5.40 ± 1.56	4.32 ± 0.24†	4.76 ± 0.72
Vcfc (circ/s)	2.9 ± 0.2	2.3 ± 0.3	2.5 ± 0.3	2.5 ± 0.2
Sa (cm/s)	2.93 ± 0.15	2.61 ± 0.21	2.84 ± 0.26	2.98 ± 0.50
Spw (cm/s)	2.94 ± 0.3	2.77 ± 0.26	3.22 ± 0.22	3.24 ± 0.22
Isovolumic relaxation time (ms)	17 ± 1	20 ± 2	19 ± 1	21 ± 1
Ea (cm/s)	4.53 ± 0.32	4.56 ± 0.37	4.74 ± 0.26	5.01 ± 0.77
Epw (cm/s)	4.34 ± 0.45	3.84 ± 0.4	4.97 ± 0.21	4.49 ± 0.49
E/Ea	20.6 ± 1.0	18.9 ± 2.5	21.6 ± 1.4	18.2 ± 2.4
Aortic regurgitation frequency	0/8	2/8	2/7	3/5

Values are mean ± SEM. †Significant difference with 5- to 7-month-old animals of the same genotype (†$p \leq 0.05$; ‡$p = 0.056$). Compliance is a local estimation calculated from the Δdiameter/Δpressure between systolic and diastolic values. LVEDD = left ventricle end diastolic diameter; Vcfc = mean shortening velocity of circumferential fibres, corrected for time (= FS/rate-corrected ejection time); Sa, Spw = maximal systolic velocity of the mitral annulus and posterior wall, respectively; Ea, Epw = maximal diastolic velocity of the mitral annulus and posterior wall, respectively. E/Ea = maximal velocity of LV mitral inflow to Ea. *Significant difference with *Fbn1*$^{+/+}$ animals of matching age.

also identified in some adult (2 out of 8) and some old (3 out of 5) *Fbn1*$^{+/mg\Delta}$ mice (Table 1 and Supporting information, Supplementary Figures 1B and 1C). These aortic insufficiencies (AI) were either mild with no cardiac complications or severe with a consistent pattern of left ventricle (LV) dysfunction (as evidenced by signs of LV remodelling, such as dilation and wall thickening leading to hypertrophy) affecting both ventricular contraction and relaxation. On the contrary, in non-symptomatic (= non-AI/non-aneurysmal) *Fbn1*$^{+/mg\Delta}$ mice, cardiac dimensions and function were not modified. The variability within the *Fbn1*$^{+/mg\Delta}$ mice, ie the presence of both clearly pathological and relatively unaffected animals, leads to a trend of structural and functional cardiac alterations in this group regarding some parameters, eg left ventricle end diastolic diameters and left ventricle weight to body weight ratios (Table 1). Collectively, these *in vivo* data suggested that the mgΔ mutation accelerates some aspects of the physiological process of vascular ageing and also leads to pathological vascular ageing to different degrees in heterozygous mutant mice. Phenotypic heterogeneity of genetically identical *Fbn1*$^{+/mg\Delta}$ mice resembles the clinical variability of MFS.

Ascending aorta morphology

Histological examination of the ascending aortae documented significant disorganization of the medial layer in *Fbn1*$^{+/mg\Delta}$ mice of all ages, which is characterized by thinner and often disrupted elastic lamellae (Figures 1C and 2, and Table 2). Interestingly, morphometric analyses also revealed that the medial layer of fibrillin-1 haploinsufficient aortae contains one less elastic lamella than normal, irrespective of the age of the mice (Table 2). This observation is consistent with the concept that has emerged from the analysis of elastin haploinsufficient mice, that the aortic wall undergoes adaptive changes in response to changes in haemodynamic stress [23,26]. Additional findings in adult and old *Fbn1*$^{+/mg\Delta}$ aortae included more diffused collagen staining, as well as histological evidence of dilation and rupture (Figures 1D and 2G, 2N, and 2U). Dissecting aneurysm was most frequently observed in tissue samples from old mutant mice in association with a more dramatic disorganization of the medial layer and fragmentation of elastic lamellae (Figures 1D and 2, and Table 2). These *in vitro* data therefore corroborated the *in vivo* evidence that microfibril deficiency in *Fbn1*$^{+/mg\Delta}$ mice causes severe architectural

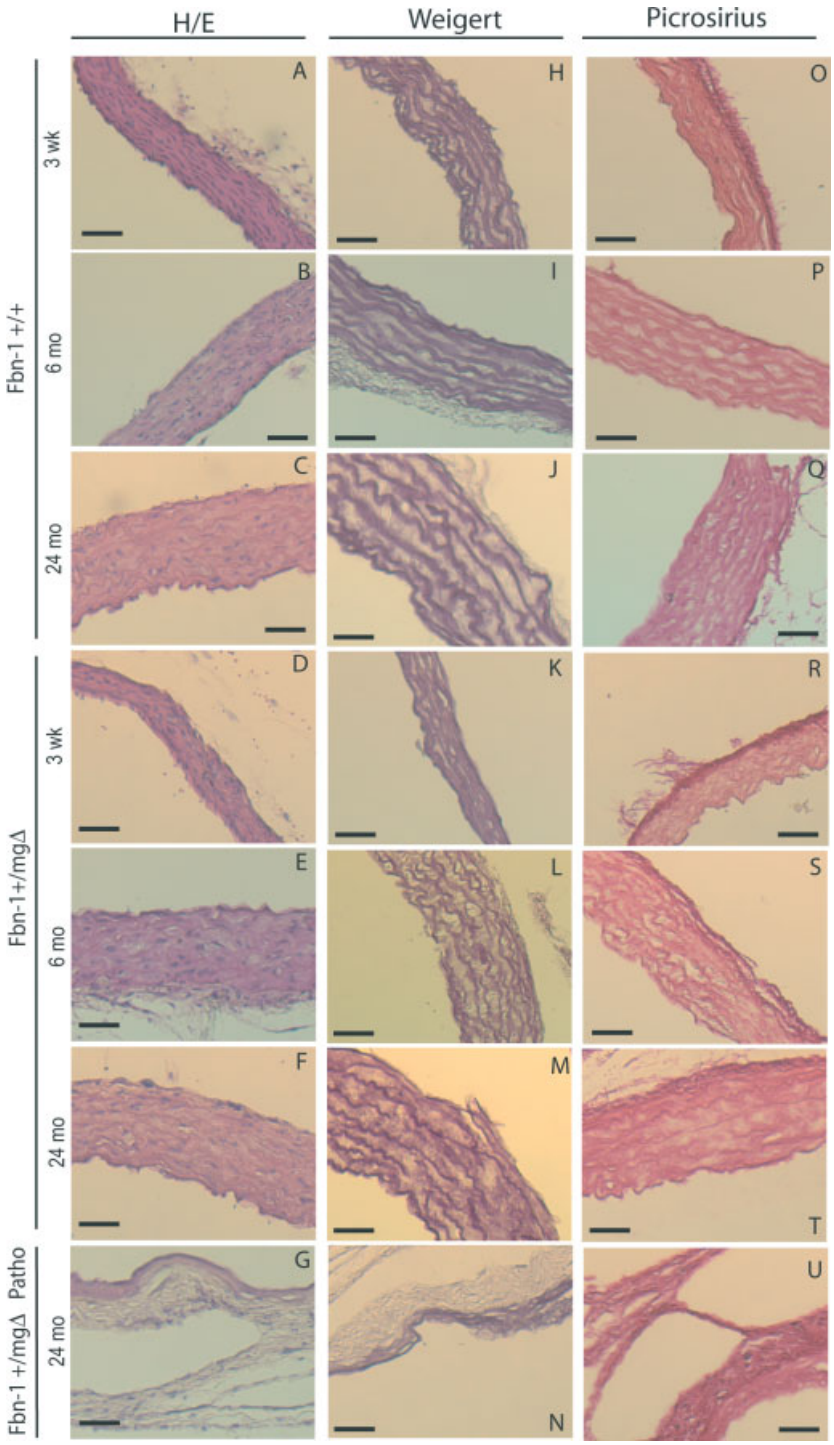

Figure 2. Histological examination of paraffin-embedded cross-sections of the ascending aorta of 3-week-old, 6- and 24-month-old *Fbn1*$^{+/+}$ and *Fbn1*$^{+/mg\Delta}$ mice, and 24-month-old pathological *Fbn1*$^{+/mg\Delta}$ mice (Patho). The elastic lamellae were thinner and disorganized in adult and aged *Fbn1*$^{+/mg\Delta}$ mice. H/E = haematoxylin/eosin staining. Bar size: 50 μm.

changes that can predispose the ageing aortic wall to structural collapse.

Ascending aorta biomechanics

In order to compare the changed structure to the function of *Fbn1*$^{+/mg\Delta}$ mouse arteries, biomechanical tests were performed on isolated aortic segments from young *Fbn1*$^{+/mg\Delta}$ mice (Figure 3). Mutant tissues displayed increased diameter, strain, and wall thickness without appreciable changes in wall stress and incremental elastic modulus (Einc). They also documented that aortae from young *Fbn1*$^{+/mg\Delta}$ mice are capable of higher extension at an imposed pressure below 100 mmHg and lower extension at an imposed pressure above 125 mmHg, compared with aortae from WT mice (Figure 3G). In adult and aged animals, the outer and inner diameters were higher and showed a greater age-related enlargement in *Fbn1*$^{+/mg\Delta}$ mice,

Table 2. Histomorphometric parameters of ascending aorta wall

Age:	3 weeks		6 months		24 months	
Genotype:	*Fbn1*$^{+/+}$	*Fbn1*$^{+/mg\Delta}$	*Fbn1*$^{+/+}$	*Fbn1*$^{+/mg\Delta}$	*Fbn1*$^{+/+}$	*Fbn1*$^{+/mg\Delta}$
Number of elastic lamellae (EL)	7.1 ± 0.3	6.1 ± 0.2*	7.7 ± 0.5	7.1 ± 0.4*	8.4 ± 0.3	6.7 ± 0.9*
Distance between EL (μm)	0.85 ± 0.34	0.70 ± 0.27	0.92 ± 0.24	1.18 ± 0.37*	0.96 ± 0.19	1.23 ± 0.6*
Rupture of EL ($\times 10^{-4}$ per μm^2)	2 ± 1	4 ± 2.8*	2 ± 1.4	6 ± 2*	3.2 ± 2.1	7.8 ± 3.6*

Values are mean ± SEM. *Significant difference between *Fbn1*$^{+/+}$ and *Fbn1*$^{+/mg\Delta}$ mice of matching age.

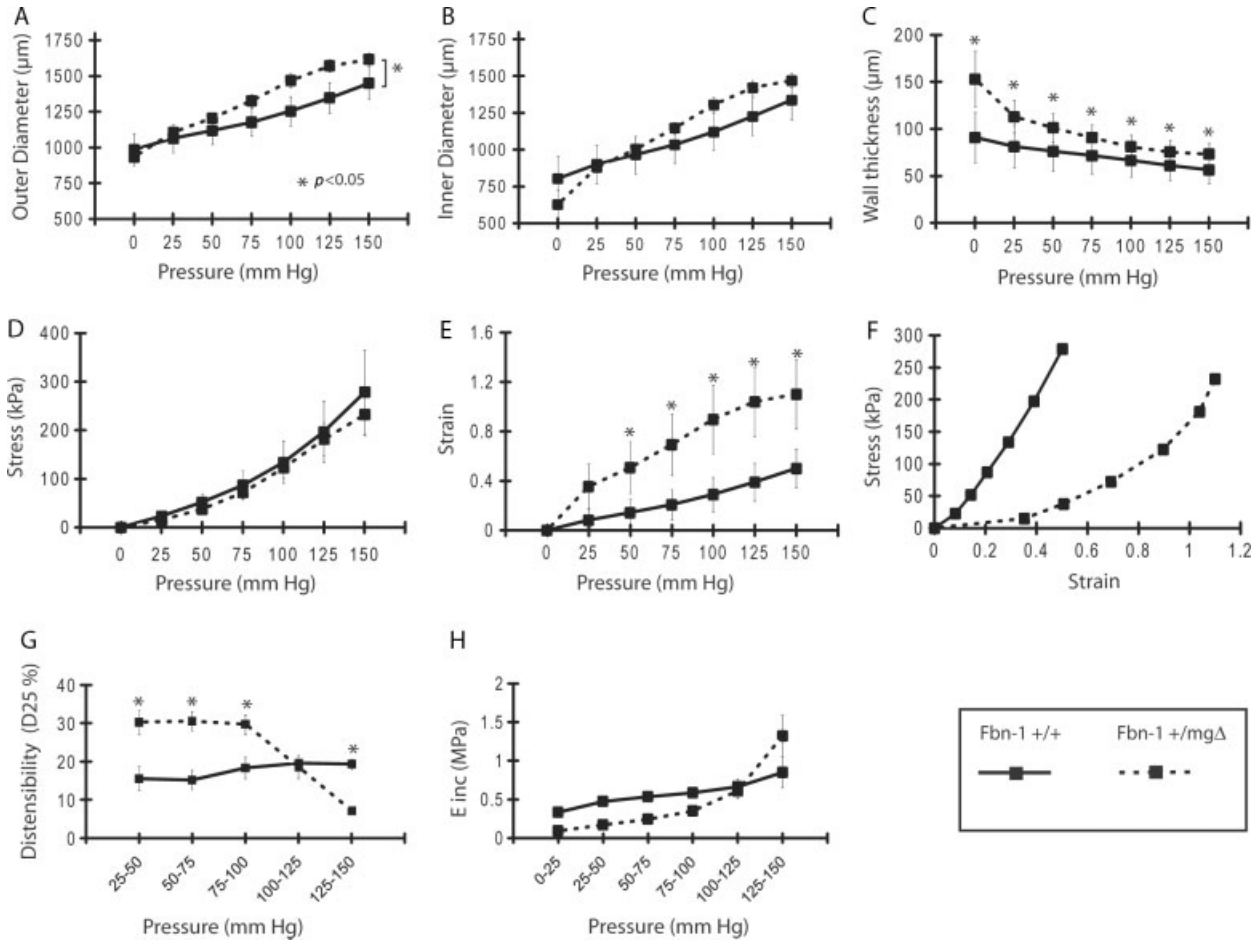

Figure 3. Diameter–pressure curves and derived mechanical parameters of the ascending aorta of 3-week-old *Fbn1*$^{+/+}$ and *Fbn1*$^{+/mg\Delta}$ mice. *Significant difference between *Fbn1*$^{+/+}$ and *Fbn1*$^{+/mg\Delta}$ mice. $n = 4–7$ per group.

which also showed an aortic wall thickness above normal in adults and abnormally thin in aged animals (Figures 4A–4C). Similar biphasic changes from controls were observed for aortic wall stress (σ), in that this parameter calculated at pressures above 125 mmHg is decreased in adult *Fbn1*$^{+/mg\Delta}$ mice and slightly increased in old mutant animals, compared with WT mice of matching ages (Figure 4D). This is due to the opposite evolutions of σ, during ageing, which decreased in WT mice because of wall thickening, and increases in *Fbn1*$^{+/mg\Delta}$ mice because of wall thinning (Figure 4C). Whereas no significant variances from the control were noted in the strain value (ε) of mutant aortae in adults, vascular ageing was associated with a relatively lower ε in *Fbn1*$^{+/mg\Delta}$ samples (Figures 4E and 4F). Similarly, the results showed that the ability of mutant aortae to extend at imposed pressures above 75 mmHg was relatively lower than normal at all ages, and that the Einc value was substantially greater in old mutant animals at imposed pressures above 100 mmHg (Figures 4G and 4H). Together, these results indicated that the mgΔ mutation substantially impairs the biomechanical properties of the ageing aortic wall.

Ascending aorta biochemistry

Aortic function greatly depends on the proper extracellular deposition and assembly of collagenous and elastic macro-aggregates [27]. Desmosine and hydroxyproline contents were therefore measured in *Fbn1*$^{+/mg\Delta}$ aortae to quantify elastin and collagen contents, respectively [14]. Increased hydroxyproline (collagen) levels and reduced desmosine (elastin) levels were found in mutant aortae, and both variances from normal increased with age relatively to unchanged amounts

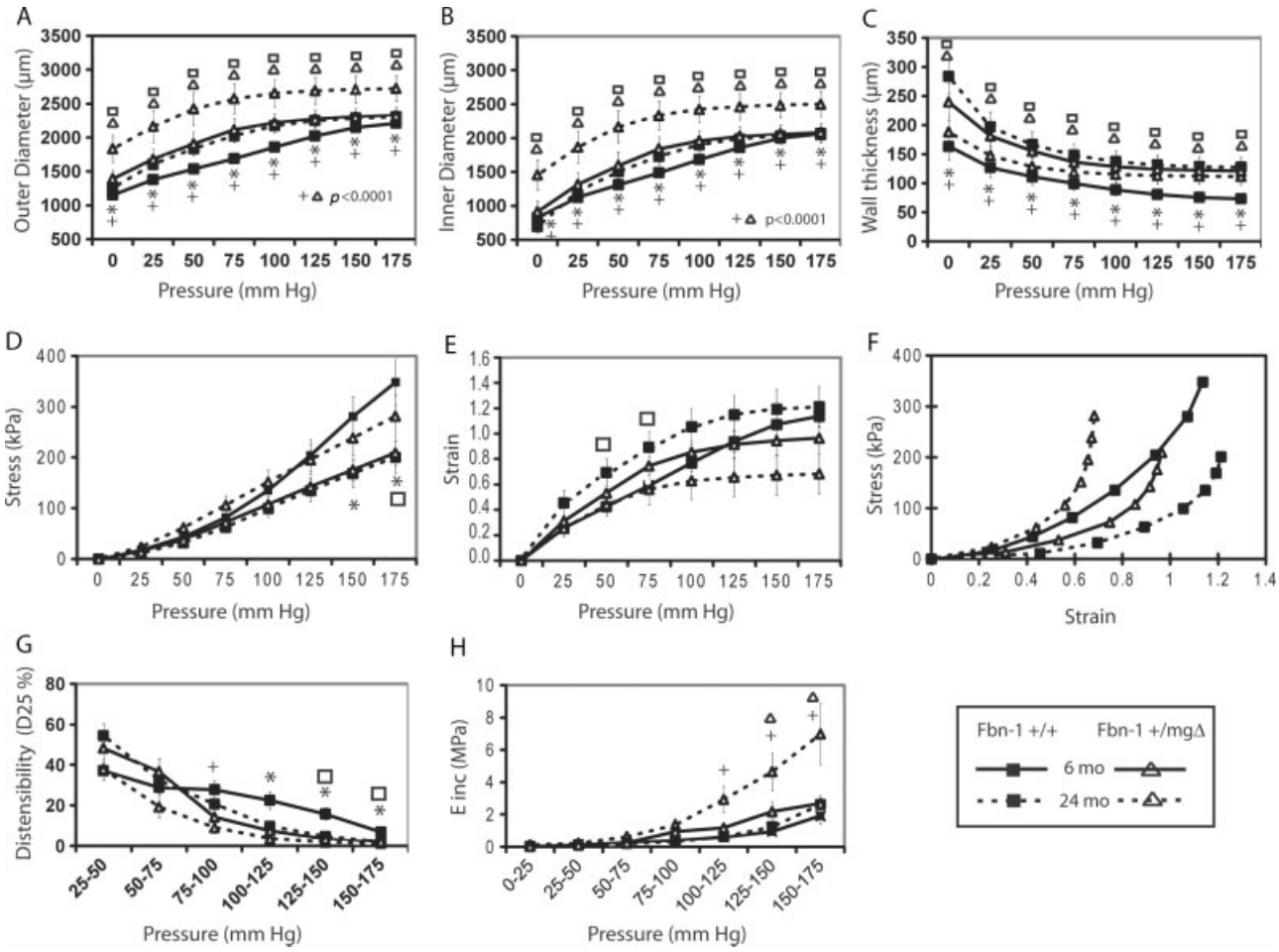

Figure 4. Diameter–pressure curves and derived mechanical parameters of the ascending aorta of 6- and 24-month-old *Fbn1*$^{+/+}$ and *Fbn1*$^{+/mg\Delta}$ mice. $^{*,+}$ Significant difference between 6-month-old *Fbn1*$^{+/+}$ and *Fbn1*$^{+/mg\Delta}$ mice or between 24-month-old *Fbn1*$^{+/+}$ and *Fbn1*$^{+/mg\Delta}$ mice, respectively. $^{\square,\Delta}$Significant difference between 6-month-old and 24-month-old values for *Fbn1*$^{+/+}$ and *Fbn1*$^{+/mg\Delta}$, respectively. $n = 5–6$ per group.

of total protein contents (Figures 5A–5E). These findings respectively corroborated the histological evidence of increased tissue remodelling and elastolysis in ageing microfibril-deficient aortae. In addition, the decreased desmosine/hydroxyproline ratio (Figure 5F) in *Fbn1*$^{+/mg\Delta}$ aortae is consistent with the decreased distensibility observed in the vessels of these adult and old animals.

Ascending aorta gene expression

The expression of key extracellular gene products, ratioed to the expression level of HPRT, was examined in the ascending aortae of young, adult, and old *Fbn1*$^{+/mg\Delta}$ mice to further support the above findings (Figures 5G–5K). As expected, *Fbn1* transcripts were significantly lower than normal (−48%) in mutant aortae of young animals and a slightly relative increase was noted in old tissues (Figure 5G). We also observed an increase in *Fbn2* expression in *Fbn1*$^{+/mg\Delta}$ animals (Figure 5H). These increases in *Fbn1* and *Fbn2* gene expression in ageing *Fbn1*$^{+/mg\Delta}$ mice might be attributed to the unproductive tissue remodelling response that is produced by smooth muscle cells in reaction to the formation of a structurally abnormal matrix. In accordance with this hypothesis, collagen I transcripts were also slightly elevated in the aortae of old *Fbn1*$^{+/mg\Delta}$ mice (decreased in young mice) (Figure 5I). Furthermore, elastin (*Eln*) transcripts were significantly lower than normal in *Fbn1*$^{+/mg\Delta}$ aortae from young animals; a similar difference was noted for lysyl oxidase (*Lox*) mRNA (Figures 5J and 5K). The same trends were confirmed when the expression of these genes was ratioed to total mRNA (Supporting information, Supplementary Figure 2). These results were consistent with the notion that *Fbn1* deficiency down-regulates the expression of other major contributors to collagen and elastic fibre assembly in early stages, while up-regulating the expression of most of these genes in late life.

Ascending aorta reactivity

Lastly, we investigated how microfibril deficiency may affect aortic tissue ability to respond to vasoconstrictor (phenylephrine, PE) and vasodilator (acetylcholine, Ach) stimuli in adult and aged animals. Response to PE, significant in *Fbn1*$^{+/+}$ mice independently of age, was decreased and became non-significant in *Fbn1*$^{+/mg\Delta}$ aortae of all ages (Figure 6A). When old

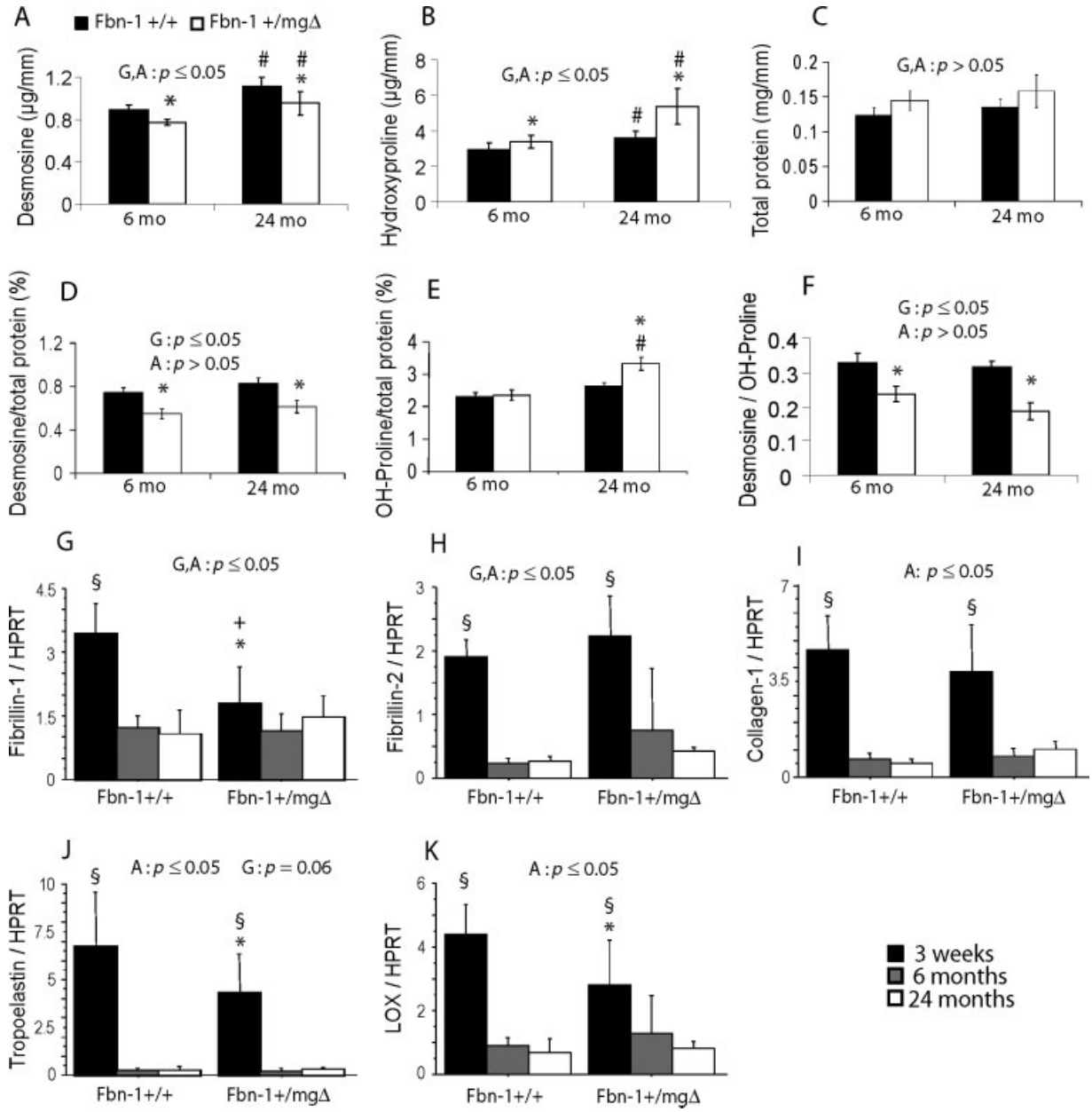

Figure 5. Desmosine and hydroxyproline contents (A–F) and elastic fibre-related gene expression (G–K) of the ascending aorta of 3-week and 6- and 24-month-old *Fbn1*$^{+/+}$ and *Fbn1*$^{+/mg\Delta}$ mice. D and E present the desmosine and hydroxyproline ratios relative to total protein content. The general effect of genotype (G) and age (A) was assessed by two-way ANOVA separately in each condition (A–K) and followed by Fisher's LSD test for paired comparisons: $^{*,\#}$ Significant difference between *Fbn1*$^{+/+}$ and *Fbn1*$^{+/mg\Delta}$ mice of the same age, and between 6- and 24-month-old mice of the same genotype, respectively. § Significant difference between young (3-week-old) on the one hand and 6- and 24-month-old animals of the same genotype on the other hand. $^{+}$ Significant difference between young (3-week-old) on the one hand and 6-month-old animals of the same genotype on the other hand. For desmosine and hydroxyproline dosages: $n = 5–7$ (6-month-old mice) and $n = 3–5$ (24-month-old mice) in each group. For mRNA expression: $n = 6$ (3-week-old), $n = 8$ (6-month-old), and $n = 5–7$ (24-month-old) in each group.

tissues were separated into non-pathological and pathological (= aneurysmal) samples, we found that the mutant aortae of the former group reacted to PE treatment more strongly than the latter group (almost no response) and equally to WT samples (Figure 6B). Non-pathological *Fbn1*$^{+/mg\Delta}$ vessels presented a lowered response to Ach (Figure 6C), independently of age, while pathological vessels could not be tested for vasorelaxation induction by Ach due to the absence of pre-constriction in response to PE. These results indicate that fibrillin-1 insufficiency alters the capacity of the aortic wall to respond to physiological vasoactive agonists.

Discussion

Elastic fibre components regulate cell proliferation, migration, and arterial morphogenesis, in addition to imparting elastic properties to blood vessels [27–32]. Interestingly, mutations in the major structural compon-

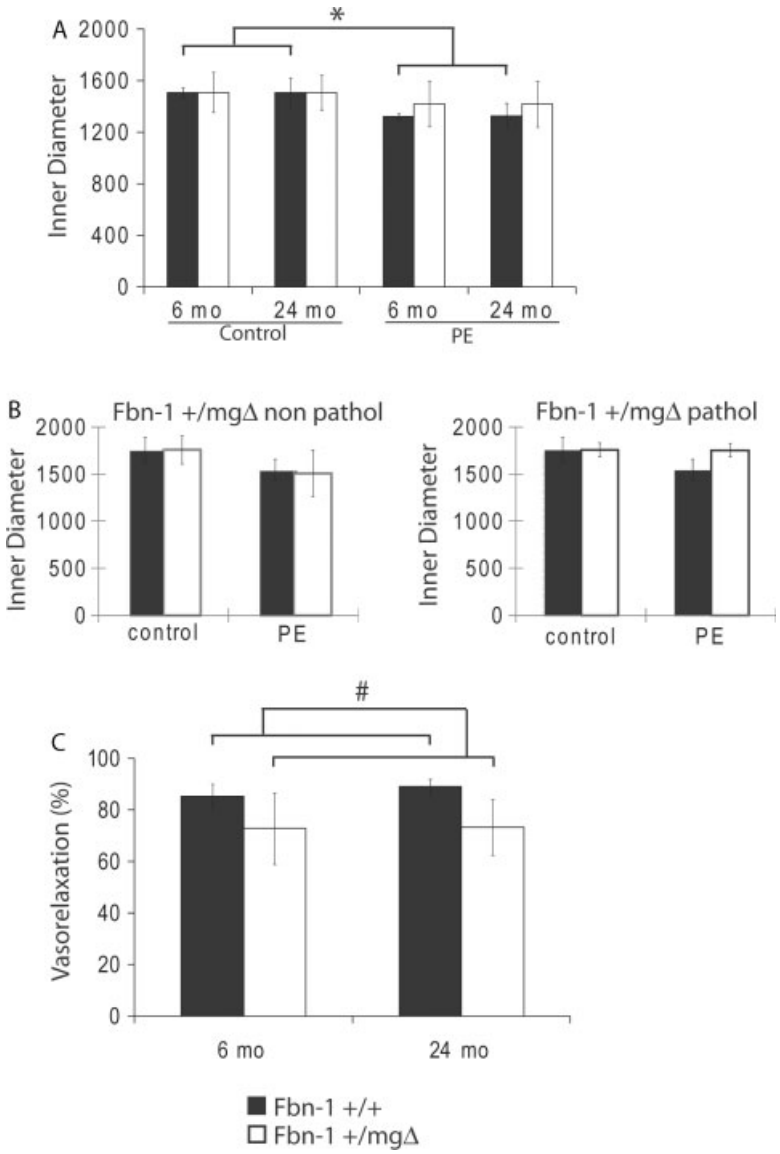

Figure 6. Reactivity to vasoactive agents of the ascending aorta of 6- and 24-month-old *Fbn1*$^{+/+}$ and *Fbn1*$^{+/mg\Delta}$ mice. (A, B) 10 µmol/l phenylephrine (PE). 24-month-old *Fbn1*$^{+/mg\Delta}$ mice were pooled (A) or separated (B) in non-pathological and pathological groups. Ach-induced vasorelaxation (10 µmol/l phenylephrine + 10 µmol/l acetylcholine) in non-pathological vessels is represented as the reversal of the PE-induced vasoconstriction, in per cent (C). *Generally significant difference with the control value, independent of age. # Generally significant difference between *Fbn1*$^{+/+}$ and *Fbn1*$^{+/mg\Delta}$ mice, independent of age. $n = 3–6$ per group.

ents of elastic fibres, elastin and fibrillin-1, have distinct vascular outcomes. On the one hand, elastin haploinsufficiency causes hyperproliferation of vascular smooth muscle cells and narrowing of large arteries in supravalvular aortic stenosis (SVAS) and Williams syndrome [33–38]. Mutations in fibrillin-1, on the other hand, cause aortic aneurysms and dissections in MFS. The opposite effects of elastin and fibrillin-1 deficiencies on vascular morphogenesis and function have been replicated in genetically engineered mouse models of SVAS and MFS. Whereas the former mutant animals have provided important insights into elastin contribution to vascular ageing, comparable information about fibrillin-1 is currently unavailable due to the fact that most studies have focused on homozygous mutant mice that die of dissecting aneurysm during the first 2 weeks of postnatal life or between 2 and 4 months of age. Here we elucidated the potential contribution of fibrillin-1 to vascular ageing in *Fbn1*$^{+/mg\Delta}$ mice that live past sexual maturity and whose adult phenotype has not been characterized. There are two major findings of our analyses.

First, ageing *Fbn1*$^{+/mg\Delta}$ mice are significantly more prone than wild-type littermates to develop dissecting aortic aneurysm. As shown in previous work, aneurysms appear earlier in *Fbn1*$^{mg\Delta/mg\Delta}$ animals, which produce only about 10% of the normal amount of fibrillin-1 [17], than in *Fbn1*$^{+/mg\Delta}$ animals, which contain about 60% of the normal content in fibrillin-1. Hence it is reasonable to argue that the presence of mutant and wild-type fibrillin-1 molecules in *Fbn1*$^{+/mg\Delta}$ mice could have a dominant negative effect on microfibril assembly, leading to the observed vasculature abnormalities. Contrasting this hypothetical

argument, however, is the factual evidence that mice underexpressing wild-type fibrillin-1 ($Fbn1^{mgR/mgR}$ mice) to nearly the same extent as $Fbn1^{+/mg\Delta}$ mice develop aortic aneurysms as well, but earlier in life (2–4 months of age) [18]. Taken together, these data strongly support the original hypothesis—that the mgΔ allele has little or no dominant negative effect on the assembly of wild-type fibrillin-1 molecules [17]. It follows that the vascular phenotype of ageing $Fbn1^{+/mg\Delta}$ mice probably reflects a gene-dosage effect that triggers aortic alterations later in life.

Ageing $Fbn1^{+/mg\Delta}$ mice are slightly hypotensive and display arteries of abnormally larger diameters and with fragmented elastic lamellae, altered mechanical properties, and reactivity, as well as increased signs of cardiac hypertrophy. These observations support the notion that microfibril deficiency modifies the process of vascular ageing in a manner opposite to elastin haploinsufficiency [14,39].

Impaired remodelling of the aortic wall in $Fbn1^{+/mg\Delta}$ mice, as evidenced by the progressive fragmentation of elastic lamellae, is likely to reflect the modified expression of at least *Fbn1, Fbn2, Eln, Lox*, and *Col1* genes, as well as enhanced matrix degradation by matrix metalloproteases (MMPs). We base the latter conclusion on published evidence of aortic elastic fibre degradation and disorganization, as well as increased MMP activity in the aortae of MFS patients and other fibrillin-1-deficient mice, and on the ability of MMP inhibition to mitigate aneurysmal progression in mouse models of MFS [6,40–42]. Expression of wild-type or mutant fibrillin-1 occurs predominantly throughout the arterial media and, to a much lower extent, in the adventitia [17]. This supports the previously articulated alternative hypothesis that increased arterial diameter and aneurysms of $Fbn1^{+/mg\Delta}$ animals reflect in part a decreased tensile strength of the adventitia, in which fibrillin-1 microfibrils may be required to properly organize the collagenous extracellular matrix during development [17]. In this view, the mutant artery would be unable to accommodate the intraluminal blood pressure and would abnormally inflate.

The fact that vascular disease in $Fbn1^{+/mg\Delta}$ mice, our model of MFS, progresses at a slower pace than in MFS patients probably reflects the lower mechanical constraints in the aortic wall of these mammalian species. In this regard, it is worth noting that a delay in the emergence of vascular abnormalities was also observed in $Eln^{+/-}$ mice, in which, unlike SVAS and Williams patients, there is no appreciable arterial stenosis even though they display an increased number of thinner lamellar units, cardiac hypertrophy, arteries of smaller diameter, and decreased elastin content, hypertension, and altered mechanics [14,23,26].

The above findings clearly indicate that fibrillin-1 is an important structural and instructive determinant of arterial wall morphogenesis, mechanical compliance, and tissue homeostasis. It is conceivable to argue that some of these functions are accounted for by the role of microfibrils in regulating cell performance through the interaction of fibrillin-1 with cell surface receptors, such as integrins and heparan sulphate proteoglycans, and latent TGFβ complexes. For example, fibrillin-1 triggers integrin-mediated signalling, which may regulate the adhesion and spreading of vascular smooth muscle cells (VSMCs) that could be required for the proper organization of aortic tissue during development [43,44]. Furthermore, improper activation of TGF signalling, as a result of impaired sequestration of latent complexes in the extracellular matrix, could also promote changes in VSMC phenotype. Moreover, it has recently been shown that fibrillin-1 fragments and microfibrils, which can pass through the basement membrane and anchor the endothelial cells to the internal elastic lamina [45], trigger integrin-mediated calcium signalling in endothelial cells [46], whose dysfunction has clearly been involved in the pathogenesis of Marfan syndrome [41,47]. A decrease in fibrillin-1 signalling, in mutant mice or human patients, could cause abnormal endothelial function and signalling to the medial VSMCs, and subsequent arterial wall dysorganization. Such endothelial dysfunction, ie impaired response to acetylcholine, was evidenced in $Fbn1^{+/mg\Delta}$ mice in our experiments. Along the same lines, the decreased number of elastic lamellae in adult $Fbn1^{+/mg\Delta}$ aortae could be viewed as a change in the remodelling capacity of $Fbn1^{+/mg\Delta}$ VSMCs that in turn reflects changes in the biosynthetic properties of these cells due to impaired cell–matrix interactions and/or latent TGFβ sequestration.

The finding that ageing $Fbn1^{+/mg\Delta}$ mice can display either seemingly normal arteries, except for some modified parameters (diameter enlargement, larger wall thickness, higher stiffness), or enhanced aneurysms, cardiac hypertrophy, and aortic insufficiency suggests that, similarly to MFS patients, fibrillin-1 mutations have varied penetrance in this mouse model. In our genetically identical animals, these phenotypic variances likely involve epigenetic or environmental factors. More generally, our data imply that accumulation of age-related environmental insults that affect the aortic wall microenvironment may disrupt cell-matrix interactions, with the consequence of accelerating the physiological process of aortic tissue degradation. In this view, mutations (even sub-clinical mutations) that affect molecules involved in elastogenesis or elastic fibre interactions with structural, cellular or soluble molecules would be expected to predispose aortic tissues to late-onset pathologies and/or premature ageing.

Acknowledgment

We acknowledge the support of the European Commission (contracts TELASTAR, 5th PCRD, No QLK6-CT-2001-00332; and ELAST-AGE, 6th PCRD, No LSHM-CT-2005-018960), the French Ministry of Foreign Affairs-EGIDE (fellowship to B Mariko), the

Association Française contre les Myopathies, the Association 'Autour des Williams', and the National Institutes of Health (AR049698).

Author contribution statement

MB and FG conceived and carried out experiments, and analysed data. HP and RF conceived experiments. PM, EB, BS, AJP, SB, QD, and JMP carried out experiments. All authors were involved in writing the paper and had final approval of the submitted and published versions.

References

1. Belz GG. Elastic properties and Windkessel function of the human aorta. *Cardiovasc Drugs Ther* 1995; **9**: 73–83.
2. Faury G. Function–structure relationship of elastic arteries in evolution: from microfibrils to elastin and elastic fibres. *Pathol Biol (Paris)* 2001; **49**: 310–325.
3. Kielty CM, Baldock C, Lee D, *et al*. Fibrillin: from microfibril assembly to biomechanical function. *Philos Trans R Soc London Ser B Biol Sci* 2002; **357**: 207–217.
4. Kielty CM, Sherratt MJ, Shuttleworth CA. Elastic fibres. *J Cell Sci* 2002; **115**: 2817–2828.
5. Adams JN, Brooks M, Redpath TW, *et al*. Aortic distensibility and stiffness index measured by magnetic resonance imaging in patients with Marfan's syndrome. *Br Heart J* 1995; **73**: 265–269.
6. Ahimastos AA, Aggarwal A, D'Orsa KM, *et al*. Effect of perindopril on large artery stiffness and aortic root diameter in patients with Marfan syndrome: a randomized controlled trial. *J Am Med Assoc* 2007; **298**: 1539–1547.
7. Baumgartner D, Baumgartner C, Matyas G, *et al*. Diagnostic power of aortic elastic properties in young patients with Marfan syndrome. *J Thorac Cardiovasc Surg* 2005; **129**: 730–739.
8. Jeremy RW, Huang H, Hwa J, *et al*. Relation between age, arterial distensibility, and aortic dilatation in the Marfan syndrome. *Am J Cardiol* 1994; **74**: 369–373.
9. Vitarelli A, Conde Y, Cimino E, *et al*. Aortic wall mechanics in the Marfan syndrome assessed by transesophageal tissue Doppler echocardiography. *Am J Cardiol* 2006; **97**: 571–577.
10. Dietz HC, Cutting GR, Pyeritz RE, *et al*. Marfan syndrome caused by a recurrent *de novo* missense mutation in the fibrillin gene. *Nature* 1991; **352**: 337–339.
11. Faury G, Chabaud A, Ristori MT, *et al*. Effect of age on the vasodilatory action of elastin peptides. *Mech Ageing Dev* 1997; **95**: 31–42.
12. Faury G, Garnier S, Weiss AS, *et al*. Action of tropoelastin and synthetic elastin sequences on vascular tone and on free Ca^{2+} level in human vascular endothelial cells. *Circ Res* 1998; **82**: 328–336.
13. Jacob MP. Extracellular matrix remodeling and matrix metalloproteinases in the vascular wall during aging and in pathological conditions. *Biomed Pharmacother* 2003; **57**: 195–202.
14. Pezet M, Jacob MP, Escoubet B, *et al*. Elastin haploinsufficiency induces alternative aging processes in the aorta. *Rejuvenation Res* 2008; **11**: 97–112.
15. Carta L, Pereira L, Arteaga-Solis E, *et al*. Fibrillins 1 and 2 perform partially overlapping functions during aortic development. *J Biol Chem* 2006; **281**: 8016–8023.
16. Judge DP, Biery NJ, Keene DR, *et al*. Evidence for a critical contribution of haploinsufficiency in the complex pathogenesis of Marfan syndrome. *J Clin Invest* 2004; **114**: 172–181.
17. Pereira L, Andrikopoulos K, Tian J, *et al*. Targeting of the gene encoding fibrillin-1 recapitulates the vascular aspect of Marfan syndrome. *Nature Genet* 1997; **17**: 218–222.
18. Pereira L, Lee SY, Gayraud B, *et al*. Pathogenetic sequence for aneurysm revealed in mice underexpressing fibrillin-1. *Proc Natl Acad Sci U S A* 1999; **96**: 3819–3823.
19. Parlakian A, Charvet C, Escoubet B, *et al*. Temporally controlled onset of dilated cardiomyopathy through disruption of the SRF gene in adult heart. *Circulation* 2005; **112**: 2930–2939.
20. Royer A, van Veen TA, Le Bouter S, *et al*. Mouse model of SCN5A-linked hereditary Lenegre's disease: age-related conduction slowing and myocardial fibrosis. *Circulation* 2005; **111**: 1738–1746.
21. Starcher B, Conrad M. A role for neutrophil elastase in the progression of solar elastosis. *Connect Tissue Res* 1995; **31**: 133–140.
22. Brown-Augsburger P, Tisdale C, Broekelmann T, *et al*. Identification of an elastin cross-linking domain that joins three peptide chains. Possible role in nucleated assembly. *J Biol Chem* 1995; **270**: 17778–17783.
23. Faury G, Pezet M, Knutsen RH, *et al*. Developmental adaptation of the mouse cardiovascular system to elastin haploinsufficiency. *J Clin Invest* 2003; **112**: 1419–1428.
24. Franc S, Garrone R, Bosch A, *et al*. A routine method for contrasting elastin at the ultrastructural level. *J Histochem Cytochem* 1984; **32**: 251–258.
25. Neptune ER, Frischmeyer PA, Arking DE, *et al*. Dysregulation of TGF-beta activation contributes to pathogenesis in Marfan syndrome. *Nature Genet* 2003; **33**: 407–411.
26. Li DY, Faury G, Taylor DG, *et al*. Novel arterial pathology in mice and humans hemizygous for elastin. *J Clin Invest* 1998; **102**: 1783–1787.
27. Wagenseil JE, Mecham RP. New insights into elastic fiber assembly. *Birth Defects Res C Embryo Today* 2007; **81**: 229–240.
28. Dietz HC, Mecham RP. Mouse models of genetic diseases resulting from mutations in elastic fiber proteins. *Matrix Biol* 2000; **19**: 481–488.
29. Maki JM, Rasanen J, Tikkanen H, *et al*. Inactivation of the lysyl oxidase gene Lox leads to aortic aneurysms, cardiovascular dysfunction, and perinatal death in mice. *Circulation* 2002; **106**: 2503–2509.
30. Nakamura T, Lozano PR, Ikeda Y, *et al*. Fibulin-5/DANCE is essential for elastogenesis *in vivo*. *Nature* 2002; **415**: 171–175.
31. Urban Z, Riazi S, Seidl TL, *et al*. Connection between elastin haploinsufficiency and increased cell proliferation in patients with supravalvular aortic stenosis and Williams–Beuren syndrome. *Am J Hum Genet* 2002; **71**: 30–44.
32. Li DY, Brooke B, Davis EC, *et al*. Elastin is an essential determinant of arterial morphogenesis. *Nature* 1998; **393**: 276–280.
33. Curran ME, Atkinson DL, Ewart AK, *et al*. The elastin gene is disrupted by a translocation associated with supravalvular aortic stenosis. *Cell* 1993; **73**: 159–168.
34. Ewart AK, Jin W, Atkinson D, *et al*. Supravalvular aortic stenosis associated with a deletion disrupting the elastin gene. *J Clin Invest* 1994; **93**: 1071–1077.
35. Ewart AK, Morris CA, Atkinson D, *et al*. Hemizygosity at the elastin locus in a developmental disorder, Williams syndrome. *Nature Genet* 1993; **5**: 11–16.
36. Ewart AK, Morris CA, Ensing GJ, *et al*. A human vascular disorder, supravalvular aortic stenosis, maps to chromosome 7. *Proc Natl Acad Sci U S A* 1993; **90**: 3226–3230.
37. Li DY, Toland AE, Boak BB, *et al*. Elastin point mutations cause an obstructive vascular disease, supravalvular aortic stenosis. *Hum Mol Genet* 1997; **6**: 1021–1028.

38. Olson TM, Michels VV, Urban Z, *et al*. A 30 kb deletion within the elastin gene results in familial supravalvular aortic stenosis. *Hum Mol Genet* 1995; **4**: 1677–1679.
39. Carta L, Wagenseil JE, Knutsen RH, *et al*. Discrete contributions of elastic fiber components to arterial development and mechanical compliance. *Arterioscl Thromb Vasc Biol* 2009; **29**: 2083–2089.
40. Xiong W, Knispel RA, Dietz HC, *et al*. Doxycycline delays aneurysm rupture in a mouse model of Marfan syndrome. *J Vasc Surg* 2008; **47**: 166–172; discussion 172.
41. Chung AW, Au Yeung K, Cortes SF, *et al*. Endothelial dysfunction and compromised eNOS/Akt signaling in the thoracic aorta during the progression of Marfan syndrome. *Br J Pharmacol* 2007; **150**: 1075–1083.
42. Chung AW, Yang HH, Yeung KA, *et al*. Mechanical and pharmacological approaches to investigate the pathogenesis of Marfan syndrome in the abdominal aorta. *J Vasc Res* 2008; **45**: 314–322.
43. Bax DV, Bernard SE, Lomas A, *et al*. Cell adhesion to fibrillin-1 molecules and microfibrils is mediated by alpha 5 beta 1 and alpha v beta 3 integrins. *J Biol Chem* 2003; **278**: 34605–34616.
44. Williamson MR, Shuttleworth A, Canfield AE, *et al*. The role of endothelial cell attachment to elastic fibre molecules in the enhancement of monolayer formation and retention, and the inhibition of smooth muscle cell recruitment. *Biomaterials* 2007; **28**: 5307–5318.
45. Davis EC. Immunolocalization of microfibril and microfibril-associated proteins in the subendothelial matrix of the developing mouse aorta. *J Cell Sci* 1994; **107**: 727–736.
46. Mariko B, Ghandour Z, Raveaud S, *et al*. Microfibrils and fibrillin-1 induce integrin-mediated signaling, proliferation and migration in human endothelial cells. *Am J Physiol Cell Physiol* 2010; **299**: C977–C987.
47. Wilson DG, Bellamy MF, Ramsey MW, *et al*. Endothelial function in Marfan syndrome: selective impairment of flow-mediated vasodilation. *Circulation* 1999; **99**: 909–915.

SUPPORTING INFORMATION ON THE INTERNET

The following supporting information may be found in the online version of this article.

Supplementary methods. Detailed materials and methods regarding ultrasound, aorta mechanics, and RNA analyses.

Figure S1. Ultrasound. A: *In vivo* arterial diameter at the level of the ascending aorta. Measurements of systolic (sd) and diastolic (dd) diameters are gated on the ECG signal in time–motion mode. B, C: Continuous wave Doppler images from the apical two-chamber view.

Figure S2. mRNA. Specific mRNA levels relative to total mRNA.